Charting a Map through the Cellular Reprogramming Landscape

Lu Wen[1,*] and Fuchou Tang[1,*]
[1]Biodynamic Optical Imaging Center, School of Life Sciences, Peking University, Beijing 100871, China
*Correspondence: wenlu.wl@gmail.com (L.W.), tangfuchou@pku.edu.cn (F.T.)
http://dx.doi.org/10.1016/j.stem.2015.02.010

Analysis of the molecular mechanisms underlying somatic cell reprogramming into iPSCs is hampered by low efficiency of conversion and resulting cellular heterogeneity. In this issue of *Cell Stem Cell*, Zunder et al. (2015) utilize mass cytometry to perform high-throughput, single-cell analyses and provide a detailed molecular roadmap of the reprogramming process.

The reprogramming of somatic cells into induced pluripotent stem cells (iPSCs) provides opportunities to carefully study mechanisms underlying flexibility and reversibility of cell fate determination (Sánchez Alvarado and Yamanaka, 2014). However, the low efficiency of conversion and high heterogeneity within the induced cell population raises significant challenges for performing such analyses. The characteristics of the small percentage of successfully reprogrammed cells during their transition to pluripotency are largely concealed by their incompletely converted counterparts when populations are analyzed as a whole. Therefore, a technique that can both examine the expression of many genes at single-cell resolution and analyze a large number of single cells cost-effectively is highly desired.

In this issue of *Cell Stem Cell*, Zunder et al. applied single-cell mass cytometry to trace the reprogramming process in great detail (Zunder et al., 2015). This technique is a variation of traditional fluorescent flow cytometry; instead of measuring fluorescence, specific antibodies are conjugated to rare metal isotopes that are then detected via atomic mass spectrometry (Bandura et al., 2009). As single-cell mass cytometry minimizes interference due to spectral overlap, this technique allows simultaneous detection of over 40 different parameters in individual cells, compared with < 12 parameters in traditional fluorescent flow cytometry. The authors further developed computational tools for visualization of these data in two dimensional space to map the progression of single cells along the reprogramming process. To further capitalize on the high-throughput advantages of the mass cytometry approach, the authors also utilized an elegant mass-tag cellular barcoding strategy that allows dozens of different samples to be pooled together, processed, and analyzed in a single tube. This minimizes potential bias arising from variations in handling different batches of samples (Bodenmiller et al., 2012). Thus, this technique allows both high-throughput and high-content analysis of the reprogramming process at the single-cell level.

Zunder et al. (2015) examined sixteen time points during somatic cell reprogramming in three different inducible systems, including one primary mouse embryonic fibroblast (MEF) and two secondary MEF reprogramming systems, to obtain a continual and detailed molecular roadmap of the reprogramming process at single-cell resolution. Despite the differences in stoichiometric expression of reprogramming factors in these three systems, visualization of the datasets from these approaches revealed striking commonalities, suggesting that there is a general molecular route that cells follow during the reprogramming process from MEFs to iPSCs. A prominent $Oct4^{high}$ $Klf4^{high}$ subpopulation was found at an early time point of the process. Although Oct4 and Klf4 have well-documented roles during the early stages of reprogramming (Radzisheuskaya and Silva, 2014; Li et al., 2010), the clear visualization of this cell population early in the continual roadmap highlights the importance of these factors in the initial stages of iPSC generation. The authors also confirmed previous findings that the mesenchymal-epithelial transition (MET) is a critical step during reprogramming of mesenchymal cells, including MEFs, into iPSCs (Li et al., 2010). Their results further suggest that incompletely reprogrammed cells are trapped between the $Oct4^{high}Klf4^{high}$ state and the completion of MET, and this partial reprogramming state was characterized by a transient surface marker $CD73^{high}CD104^{high}$ $CD54^{low}$ pattern.

Later reprogramming stages were shown to involve activation of endogenous Nanog expression, followed by a bifurcation into bona fide iPSCs or an alternate endpoint population. The cells in this abundant, alternative final cell population expressed lower levels of pluripotency genes, including Oct4, Sox2, and Nanog, and appeared to acquire a mesenendoderm-like state with elevated expression of Lin28 and PDGFR-α. Further investigations are required to fully characterize this alternate final state to understand the inefficiency of iPSC generation. The authors then assessed how cell signaling states may affect cell paths along this bifurcation. Since single-cell mass cytometry is based on antibody recognition, it is able to detect posttranslational modifications for analysis of cellular signaling pathways. The authors measured ten signaling-associated protein modifications and identified a burst of phospho-S6 during the later stages of reprogramming of primary MEFs, indicating activation of the PI3K/mTOR pathway. Further drug inhibition experiments demonstrated that the PI3K/mTOR pathway was indeed functionally essential for reprogramming of primary MEFs into iPSCs.

This work demonstrates the power of the mass cytometry technique for molecular dissection of a cell fate determination process, providing temporal snapshots at

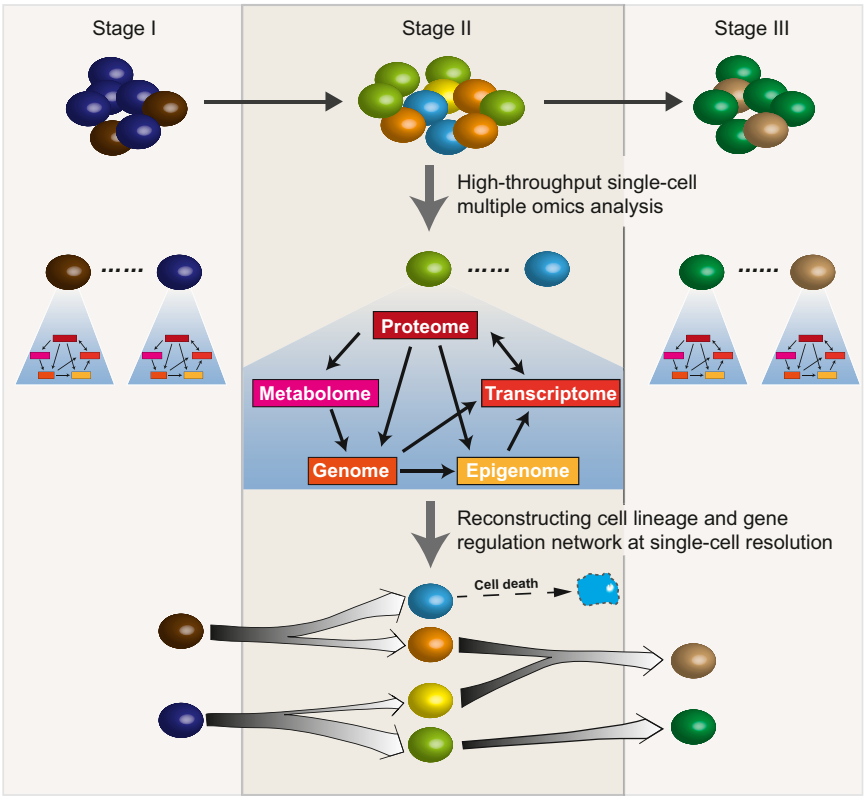

Figure 1. Reconstructing the Steps of Cellular State Changes by High-Throughput, Single-Cell Multiomics Analyses

Changes in cell state can be visualized in three stages: (I) the initial starting population; (II) transitioning, intermediate cells; and (III) the final cell population. Ideally, progression through these stages can be analyzed by putative high-throughput single-cell multiple omics technologies. In each individual cell, the genome, epigenome, transcriptome, proteome, and metabolome are simultaneously analyzed, and the intrinsic connections among these datasets are determined. When a sufficiently large number of single cells at dense enough time points are analyzed, a continual and detailed cell-lineage map of the process can be accurately reconstructed, and the gene regulation network within each individual cell will be revealed.

single-cell resolution. In the future, it should be especially useful for analysis of small molecule-based reprogramming methods and cellular transdifferentiation, in which truly reprogrammed cells are rare (Xu et al., 2015). A minor concern for single-cell mass cytometry analysis is how to distinguish technical noise from biological variations of gene expression among individual cells. One potential solution is to measure a target protein in the same single cell twice using two antibodies tagged by different isotopes, and thus the technical noise or measurement uncertainties can be accurately determined for each target protein in each individual cell.

Recent developments in single-cell RNA-seq technology have increased throughput to hundreds or even thousands of single cells, while at the same time exponentially decreasing costs (Shapiro et al., 2013). Although single-cell RNA-seq technology is still limited in terms of throughput compared to mass cytometry, its great advantage is that it measures RNA expression at whole transcriptome scale instead of a small subset of selected genes. In the future, it may be possible to combine these two complementary approaches for studying a dynamic and heterogeneous biological process. For instance, single-cell RNA-seq technology could be applied to analyze a relatively small number of single cells sorted from subpopulations of interest by FACS to screen for candidate markers or master genes. Then, a large number of cells could be sampled and intensively analyzed at serial time points by single-cell mass cytometry, using antibodies targeting the identified candidates to obtain a high-resolution roadmap. One concern of such single-cell omics analyses is that they do not provide continual cell lineage tracing, as live-cell imaging does (Hoppe et al., 2014). However, similar information can be obtained by analyzing large numbers of cells at frequent time points, as shown here by Zunder et al. (2015). Furthermore, by combining these single-cell approaches with targeted gene editing of candidate genes and mathematical modeling, interrogation and reconstruction of the gene regulation networks controlling cell-state transitions can be accomplished.

Looking forward, the ideal tools for single-cell analysis would provide both high-throughput and high-content analysis, simultaneously delivering information on multiple aspects of cell state, including the genome, epigenome, transcriptome, proteome, and metabolome, within the same individual cell (Figure 1) (Wen and Tang, 2014). Such a technology will make single cells an ideal test tube for analyzing the gene networks that regulate stem cell biology, greatly accelerating progress in the stem cell field.

REFERENCES

Bandura, D.R., Baranov, V.I., Ornatsky, O.I., Antonov, A., Kinach, R., Lou, X., Pavlov, S., Vorobiev, S., Dick, J.E., and Tanner, S.D. (2009). Anal. Chem. *81*, 6813–6822.

Bodenmiller, B., Zunder, E.R., Finck, R., Chen, T.J., Savig, E.S., Bruggner, R.V., Simonds, E.F., Bendall, S.C., Sachs, K., Krutzik, P.O., and Nolan, G.P. (2012). Nat. Biotechnol. *30*, 858–867.

Hoppe, P.S., Coutu, D.L., and Schroeder, T. (2014). Nat. Cell Biol. *16*, 919–927.

Li, R., Liang, J., Ni, S., Zhou, T., Qing, X., Li, H., He, W., Chen, J., Li, F., Zhuang, Q., et al. (2010). Cell Stem Cell *7*, 51–63.

Radzisheuskaya, A., and Silva, J.C. (2014). Trends Cell Biol. *24*, 275–284.

Sánchez Alvarado, A., and Yamanaka, S. (2014). Cell *157*, 110–119.

Shapiro, E., Biezuner, T., and Linnarsson, S. (2013). Nat. Rev. Genet. *14*, 618–630.

Wen, L., and Tang, F. (2014). Cell *157*, 771–773.

Xu, J., Du, Y., and Deng, H. (2015). Cell Stem Cell *16*, 119–134.

Zunder, E.R., Lujan, E., Goltsev, Y., Wernig, M., and Nolan, G.P. (2015). Cell Stem Cell *16*, this issue, 323–337.